Characterization of Electrical Tree Degradation of Epoxy Resin under Thermal and Temperature Stresses by Photoelastic Effect*

Hein Htet Aung[1#], *Yuhuai Wang*[1#], *Jin Li*[1*], *Ying Zhang*[2*] *and Tatsuo Takada*[3]

(1. School of Electrical and Information Engineering, Tianjin University, Tianjin 300072, China;
2. Department of Power Generation and Transformation Engineering,
Baoding Technical College of Electric Power, Baoding 071051, China;
3. Measurement and Electric Machine Control Laboratory, Tokyo City University, Tokyo 158-8557, Japan)

Abstract: Epoxy resin is widely used in the support, insulation, and packaging components of electrical equipment owing to their excellent insulation, thermal, and mechanical properties. However, epoxy-resin insulation often suffers from thermal and mechanical stresses under extreme environmental conditions and a compact design, which can induce electrical tree degradation and insulation failure in electrical equipment. In this study, the photoelastic method is employed to investigate the thermal-mechanical coupling stress dependence of the electrical treeing behavior of epoxy resin. Typical electrical tree growth morphology and stress distribution were observed using the photoelastic method. The correlation between the tree length and overall accumulated damage with an increase in mechanical stress is determined. The results show that compressive stress retards the growth of electrical trees along the electric field, while tensile stress has accelerating effects. This proves that the presence of thermal stress can induce more severe accumulated damage.

Keywords: Epoxy resin, electrical tree degradation, thermal stress, mechanical stress, photoelastic effects

1 Introduction

Epoxy resin is a broad term that refers to a polymer that contains epoxy groups. These groups can transform from a linear structure into a stable cross-linked network through a reaction with a curing agent [1-3]. Epoxy resin is commonly used in high-voltage insulation equipment, such as support insulators, cable terminals, insulation pull rods, and power module packaging. Epoxy resin has exceptional heat resistance, mechanical properties, insulation performance, and favorable processability [4-7]. However, with the development of compact designs, large-scale power transmission, and extreme environments, epoxy insulation must withstand high temperatures, mechanical and electrical stresses during operation. Combined with the local electric field concentration caused by internal defects, the insulation degradation process can be accelerated, and a rapid failure fault can decrease the reliability of electrical equipment [8-10].

With improvements in the voltage level, capacity, and integration of electrical equipment, the failure rate of epoxy insulation components is rapidly increasing, which presents higher requirements and challenges to the insulation performance of epoxy resin [11-13]. In recent years, statistics on electrical equipment accidents, both domestically and internationally, indicate that incidents of electrical tree breakdown in epoxy resin insulation components have frequently occurred under the combined effects of mechanical stress and temperature gradient fields. In 2014, a basin insulator at a substation experienced a fault breakdown [14]. The research results indicate that insulators generate small cracks owing to installation process problems, and the cracks further expand during long-term live operation, ultimately forming a discharge channel for the conductor to reach the shell. In 2016, the epoxy sleeve of a gas insulated-switchgear (GIS) terminal in a substation cracked

Manuscript received October 10, 2023; revised November 12, 2023; accepted November 20, 2023. Date of publication March 31, 2024; date of current version January 25, 2024.
# These authors contributed to this work equally.
* Corresponding Author, E-mail: lijin@tju.edu.cn, zhangying2019@tju.edu.cn
* Supported by the National Natural Science Foundation of China (52377153) and Science and Technology Project of Hebei Education Department (QN2023073).
Digital Object Identifier: 10.23919/CJEE.2023.000047

because it was in a stress state close to its material strength limit for a sustained period [15]. In September of the same year, a 500 kV three pillar gas-insulated line (GIL) at a converter station experienced a rupture fault [16]. In recent years, multiple insulation-breakdown accidents have occurred during the operation of insulated pull rods [17]. On September 28, 2016, the GIS circuit breaker of the Beijing West Station ultra-high-voltage AC project malfunctioned. During disassembly, it was discovered that the insulation rod had broken. In April 2018, the insulation rod of the Suzhou expansion station was discharged, and there were evident signs of damage to the surface of the rod. In 2016, the insulation rod at the Jinan Station experienced an insulation-breakdown failure. In December 2020, the insulation rod of the circuit breaker at the Wuhu expansion station broke, and burn marks were discovered on-site. The accident investigation revealed that complex operating conditions were the predominant cause of the deterioration of the power generation branches, leading to the breakdown failure of the epoxy insulation components.

Electrical treeing is the primary cause of the insulation-breakdown of epoxy resins, which is closely related to the partial discharge behavior of dielectrics [18]. Under the action of an electric field, space-charge trapping, detrapping, and recombination processes release energy and accelerate the degradation of the polymer molecular chain, eventually forming a low-density region [19]. With the accumulation of molecular chain damage, polarization occurs at the defects, generating polarized charges and resulting in local electric field distortion [20]. Therefore, when the critical value of the insulation-breakdown strength in this region is exceeded, multiple partial discharges can form electrical tree channels [21]. The phenomenon of electrical treeing is a crucial factor that restricts the safe and reliable operation of power equipment. It is urgent to comprehensively reveal the growth mechanism of the electrical treeing of epoxy resin insulation materials under mechanical stress and temperature gradient fields.

Significant progress has been made in understanding the electrical tree degradation characteristics of insulating materials, such as cross-linked polyethylene, silicone rubber, and ethylene propylene diene monomers, under mechanical stress or thermal gradients [18, 22]. However, the large modulus and stress concentration of the epoxy resin make it difficult to study the electrical tree degradation behavior [23]. With increasing tensile stress, the tree inception probability and growth rate increased, and branch-like trees formed easily. With increasing compressive stress, both the tree length and corresponding accumulated damage first decreased and subsequently increased. Based on the calculation results of the driving energy of electrical tree growth under electrical and mechanical stress, the growth mechanism of an electrical tree under mechanical stress was analyzed [24]. Moreover, it was found that a large temperature gradient led to an increase in the number of electrical tree channels, damage area, and results in a shorter breakdown time. The thermal stress generated by the temperature gradient changes the strain distribution of the material, reduces the energy required for the growth of the electrical tree, and promotes the development of the electrical tree [25]. However, research progress on the direct correlation between the mutual presence of thermal-mechanical coupling stress and the electrical treeing process of epoxy resin is still lacking.

Therefore, this study introduces a photoelastic method to further explore the coupling effects of thermal-mechanical stress on the electrical tree degradation process. The correlation between stress and tree growth characteristics, such as length and accumulated damage, is examined. A diagram of the electrical degradation model is established to reveal the related mechanisms.

2 Methods

2.1 Sample preparation

The test samples were composed of bisphenol-A epoxy resin HY-511 and amine curing agent HY-651 with mass ratio of 3:1, produced by Yanhai Chemical Co., Ltd. The mixture was degassed in a vacuum chamber and cast into a mold embedded with a steel needle. The samples were pre-cured at room temperature (around 20 ℃) for 48 h and then cured at 60 ℃ for 8 h. Dumbbell-type standard tensile

specimens were prepared for tensile stress tests. The narrowest part of the specimen was 50 mm long, 4 mm wide, and 3 mm thick. Rectangular specimens with dimensions of 50 mm×4 mm×3 mm were fabricated for the compression stress test. The samples were selected under the microscope, and only the samples with a needle plate distance of (2±0.1) mm were employed for the electrical treeing experiment.

2.2 Electrical tree experimental setups

The electrical tree experimental setups are shown in Fig. 1a, which include the AC power source, voltage divider, and mechanical device that can provide tensile and compressive forces. The loading rate was 30 MPa/min during the tensile and compressive stress tests. The change in the applied external force load was recorded using a force measurement system. The mechanical stress σ in the sample is defined by Eq. (1)

$$\sigma=F / bc \tag{1}$$

where F denotes the applied force of the mechanical device (N), b indicates the width of the specimen (m), and c denotes the thickness of the specimen (m).

A needle-plate electrode system with a distance of 2 mm was designed for the electrical treeing degradation tests. The applied AC voltage was set to 15 kV. Twenty samples were analyzed for each condition to ensure statistical accuracy. To study the electrical tree growth characteristics, the tree length and accumulated damage were recorded, which were obtained by calculating the total number of pixels covered by the electrical tree channel. The temperature gradient controller is shown in Fig. 1b. The temperature control system consists of heating plates, sensors, and other units. The temperature gradient was realized using ceramic heating plates on the needle electrode and grounding sides. To prevent the heat of the high-temperature side from being transmitted to the low-temperature side of the sample, an experimental device was set up with a temperature-controlled water-cooling system. Before applying the voltage, the temperature of the high-voltage side and the grounding side was maintained for 15 min to obtain a stable temperature gradient ΔT=60 ℃. The temperature of the high-voltage electrode and ground electrode of the sample was 90 ℃ and 30 ℃, respectively.

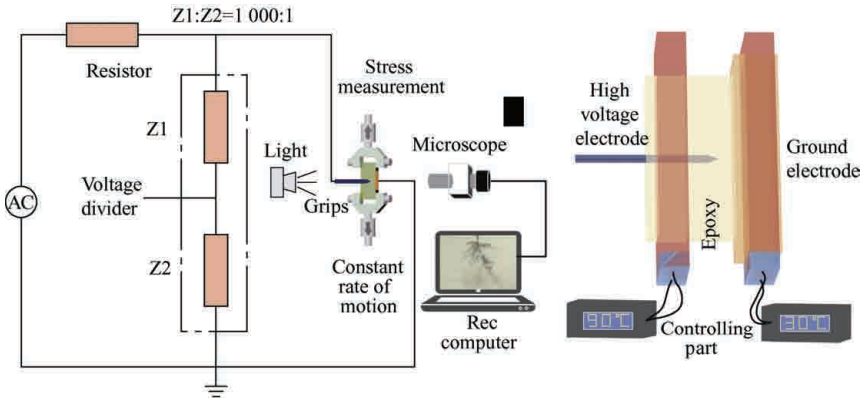

(a) Electrical degradation test (b) Temperature gradient control system

Fig. 1 Experimental setup for electrical treeing tests under thermal-mechanical coupling tresses

2.3 Mechanical stress characterization

To observe the stress distribution in the specimen, the photoelastic method shown in Fig. 2 was employed. The incident light E is decomposed into two polarized beams E_1 and E_2 with an orthogonal vibration direction when it passes through the object. The path difference between the two beams after passing through the object is Δ because the two beams travel at different speeds. The principal stress difference $\sigma_1-\sigma_2$ is calculated by Eqs. (2)-(4).

$$\sigma_1-\sigma_2=n\lambda / Ch \tag{2}$$

$$\sigma_1-\sigma_2=n\lambda / C \tag{3}$$

$$f=\lambda / C \tag{4}$$

where n indicates the fringe order, λ symbolizes the wavelength of incident light wave, C denotes the material optical sensitivity coefficient, h indicates the

sample thickness and f indicates the fringe value of material, which is usually determined by experiment. When white light was used as the light source, colored stripes appeared. When the differences in the principal stresses were equal, the stripe color was the same. Here, f, the photoelastic constant, i.e., the fringe value of the epoxy resin selected is 11 MPa • mm with λ= 490 nm [26-27]. The sample thickness, h, is 3 mm. In this study, the mechanical stress generated by the applied load was uniform across the samples. We set the position as zero stress, and the thermal stress in the other positions can be obtained using Eq. (2). This is referred to as the stress gradient generated by the temperature gradient.

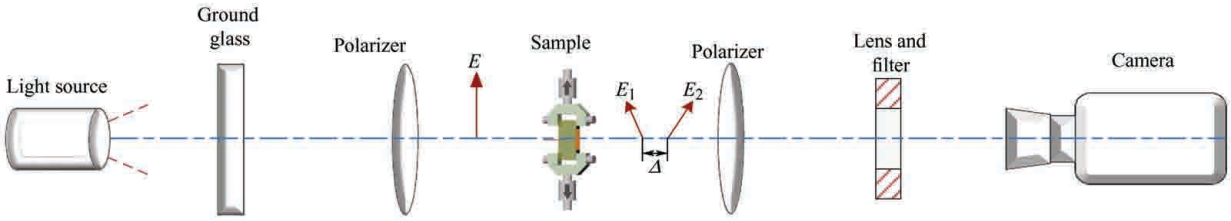

Fig. 2 Photoelastic method for observing the stress distribution

3 Results and discussion

3.1 Electrical tree degradation

The relationships among the tensile stress, electrical tree length, and accumulated damage under different temperature gradients are depicted in Fig. 3. According to Fig. 3a, when ΔT is 0 and 60 ℃ and when the tensile stress changes from 0 to 30 MPa, the average electrical tree length increases continuously, indicating that the tensile stress promotes the growth of the electrical tree along the electric field. The length of the electrical tree at 60 ℃ is much longer than that at 0 ℃, indicating that an increase in the local temperature accelerates the growth of the electrical tree.

In addition to the length of the electrical tree, the accumulated damage can be used to evaluate the overall deterioration caused by the electrical tree. Fig. 3b shows the relationship between the accumulated damage to the electrical tree and the tensile stress. When ΔT is 0 and 60 ℃, the accumulated damage increases with tensile stress. The accumulated damage at 60 ℃ is much higher than that at 0 ℃. The accumulated damage is the result of changes in the length and structure of an electrical tree. Additionally, when the tensile stress increases from 20 MPa to 30 MPa, the accumulated damage growth rate when ΔT is 0 ℃ is higher than that when ΔT is 60 ℃. Moreover, it can also be observed from the study of the mechanical stress distribution that when the temperature rise releases the stress concentration area; that is, although the applied stress increases, the internal microdefects of the epoxy resin show a reduced increase, which slows down the degree of local electric field distortion and the probability of partial discharge, thus reducing the accumulated damage rate of the electrical tree.

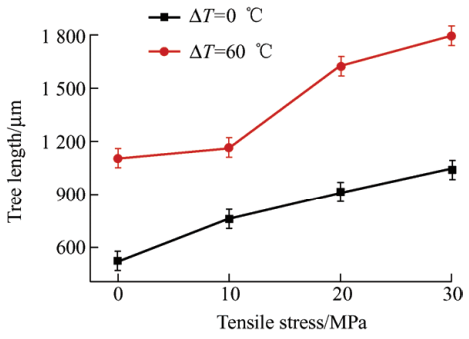

(a) Tree length

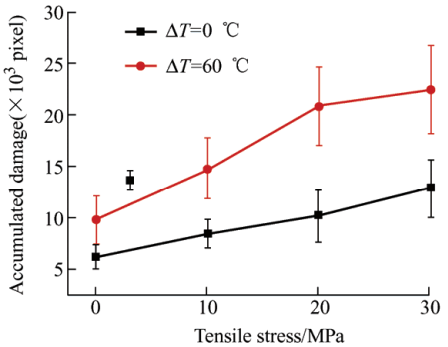

(b) Accumulated damage

Fig. 3 Tree length and accumulated damage as functions of different tensile stress

Fig. 4 depicts the relationship between the compressive stress, electrical tree length, and accumulated damage under different temperature

gradients. As shown in Fig. 4a, when the compressive stress changes from 0 to 10 MPa, the length of the electrical tree decreases. Appropriate compressive stress can increase the polymer molecular chain breakage threshold and reduce the probability of electrical dendrite initiation. When the compressive stress continues to increase, the damage to the molecular chain caused by the stress intensifies, and the micro defects in the epoxy resin increase, which generates charge accumulation inside the defects and a strong local electric field, thus accelerating the growth of the electrical tree. Compared with ΔT at 0 ℃, the electrical tree length growth at 60 ℃ is higher, which indicates that an increase in the local temperature may accelerate the growth of the electrical tree. When ΔT is 60 ℃, the length of the electrical tree is the highest, and the temperature rise near the high-voltage electrode can threaten the insulation safety.

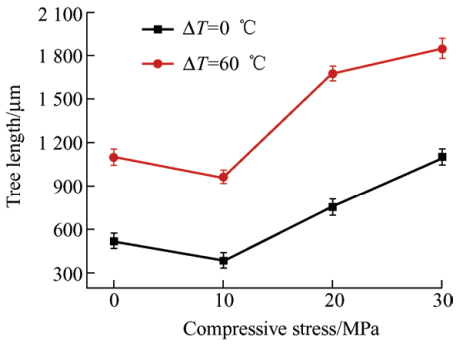

(a) Tree length

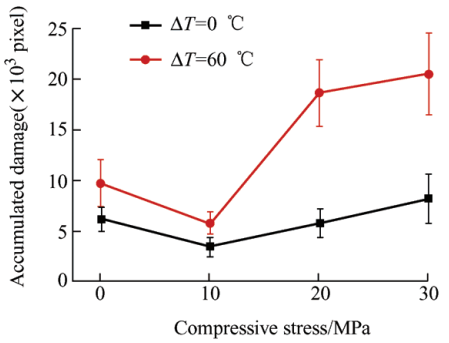

(b) Accumulated damage

Fig. 4 Tree length and accumulated damage as functions of different compressive stress

Fig. 4b shows the relationship between the accumulated damage to the electrical tree and the compressive stress. When ΔT is 0 and 60 ℃, the accumulated damage first decreases and then increases with the increase of compression stress, and the accumulated damage at 60 ℃ is much higher than that at 0 ℃. Moreover, when the compressive stress rises from 20 MPa to 30 MPa, the accumulated damage growth rate at 60 ℃ is less than that at 0 ℃. The analysis shows that the stress concentration area is released at high temperatures, and the influence of stress on the growth of the electrical tree was weakened; thus, the accumulated damage rate decreased.

3.2 Mechanical stress distribution

For comparison, the typical photoelastic images of electrical trees with the same stressing time under tensile and compressive load of 10 MPa at 90 ℃ are presented in Fig. 5. Tensile stress promotes electrical tree growth in the stress direction, forming a bush-like tree, while compressive stress causes the electrical tree to grow perpendicularly, forming a branch-like tree.

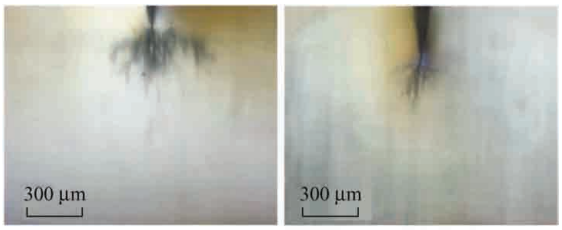

(a) Tensile stress (b) Compressive stress

Fig. 5 Typical morphologies of electrical trees at high temperatures under tensile and compressive stresses

When comparing the two scenarios, no obvious stress concentration was observed in the sample under a homogeneous temperature, even with tensile or compressive loads. To further investigate the effects of thermal stress, the high-voltage electrode and ground electrode temperatures are 90 ℃ and 30 ℃, respectively, and the temperature gradient is 60 ℃. The photoelastic images show that the stress distribution under the temperature gradient is significantly different, as shown in Figs. 6 and 7.

Fig. 6 shows the stress distribution of the needle electrode at a temperature gradient of 60 ℃ under tensile stress. According to the photoelastic images, the stress distribution was consistent throughout the process. Stress initiates from the tip of the needle electrode, becomes stronger, and extends in the direction of the applied stress, that is, perpendicular to the needle electrode. The analysis shows that under an external tensile stress, owing to the existence of the

needle tip, the stress distribution is uneven, resulting in the maximum tensile stress in front of the needle electrode. The highest stress was found in the layers along the applied stress direction, as shown in Fig. 6. Zero- or very-low-stress regions are found near the low-voltage side, that is, the high-temperature side, because the high temperature releases the stress concentration area.

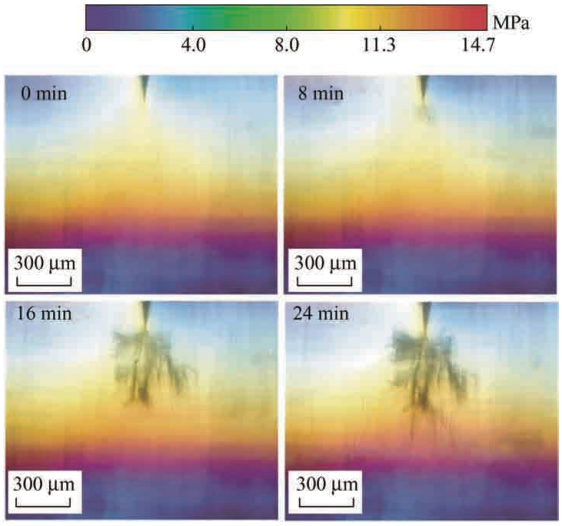

Fig. 6 Growth process of the electrical tree with T_G=60 ℃ under tensile stress

Fig. 7 shows the stress distribution of the needle electrode with a temperature gradient of 60 ℃ under compressive stress. The stress distribution was found to be contrary to that of the previous case. Following the application of compressive stress together with the temperature gradient, a relatively low amount of stress is found at the tip of the needle electrode, which then grows toward the ground electrode. The highest stress levels existed on the two sides of the needle electrode, where the thermal stress met the applied compressive stress.

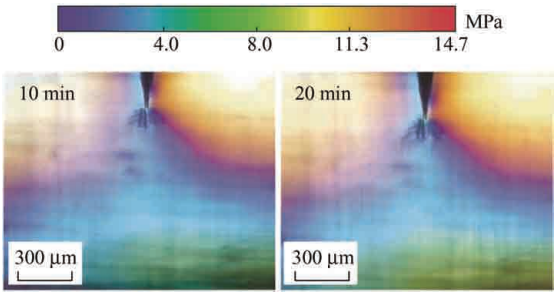

Fig. 7 Growth process of electrical tree with T_G=60 ℃ under compressive stress

When comparing the two scenarios, the most significant difference is that the stress is highly distributed along the stress directions under a tensile load, whereas the highest stress regions only exist as certain shapes near the high-voltage side in the latter. It is speculated that this is caused by the different effects of tensile and compressive stresses on the needle tip. The epoxy resin exhibits a slight deformation under mechanical stress. Under tensile stress, the position of the needle tip is equivalent to that of a notch, which did not block the tensile deformation of the epoxy tree. However, under compressive stress, the micro-deformation of the resin on both sides of the needle tip is blocked; thus, the stress distribution of the resin under tensile and compressive stresses is significantly different. Although the two scenarios show opposite phenomena in terms of stress distribution, the thermal stress still promotes the electrical tree process in both cases. Moreover, thermal-mechanical coupling stress can accelerate the process and increase the growth of the electrical tree length further than single mechanical stress.

3.3 Discussions

The relationship between the thermal and mechanical coupling stress and the electrical tree morphology is depicted in Fig. 8. In this study, the thermal-mechanical combined stress value is set as a controlling parameter and the *X*-axis. Three types of results were obtained under different conditions: a low- or zero-voltage level in the absence of a temperature gradient, a high-voltage level in the absence of a temperature gradient, and a high-voltage level with a temperature gradient. When the tree length is greater than zero, it indicates that an electrical tree can be generated; the larger the value, the more severe the degradation of the electrical tree. When the tree length is less than zero, the opposite occurs. In the absence of a temperature gradient, when the applied voltage is not sufficiently large and the mechanical stress is low, an electrical tree does not occur. With an increase in the mechanical stress, the probability of electrical tree initiation increases. When the voltage is sufficiently high, an electrical tree is more likely to initiate and grow as the tensile stress increases. When the compressive stress increases, electrical tree growth exhibits a nonlinear trend. This explains the variation

pattern shown in Fig. 4, where an appropriate compressive stress can suppress the tree growth process. When a temperature gradient of 60 ℃ is applied, the breakdown process becomes even faster, and the curve is found to be steeper. This proves that thermal stress in superposition with mechanical stress has a stronger effect on the electrical tree formation process. Moreover, it can be observed that under the same temperature gradient, the tensile and compressive stresses show different tree-growth morphologies.

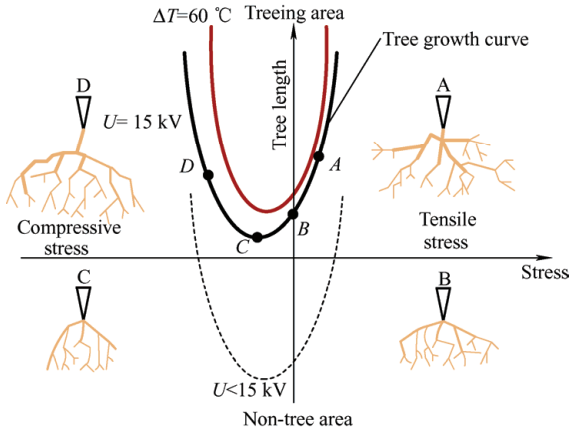

Fig. 8 Relationship between electrical tree morphology and thermal-mechanical stress

As shown in the first and fourth quadrants of Fig. 8, electrical tree growth accelerates with an increase in tensile stress, while the temperature gradient promotes the process. As a result, the breakdown time becomes shorter, and the accumulated damage rate increases significantly. In the second and third quadrants, compressive stress can initially inhibit tree growth; however, once the stress exceeds a certain value, the growth of the electrical tree is accelerated, and the temperature gradient further promotes the process. According to the curve, tensile stress consistently accelerates tree growth, while compressive stress initially decelerates the process and then accelerates it after reaching a certain point. However, thermal stress promotes the growth process in any event and induces more severe damage in a relatively short period. This is consistent with the results presented in Section 3.1.

In the absence of a temperature gradient, the electrical tree tends to exist as a small bush- or branch-like structure at low voltages. At this time, the breakdown process is only in the initiation stage; the tree branches are still short, and the effects are not significant. However, when the voltage level is increased and thermal stress is applied together with the already present mechanical stress, the tree process becomes more severe. Tree branches grow faster in certain directions to form more complex structures, which may lead to the formation of cracks and voids in the epoxy resin. This is consistent with the results presented in Section 3.2.

4 Conclusions

The following conclusions were drawn from this study.

(1) Under high mechanical stress, the electrical tree exhibits a sparser structure and larger destructive area. Tensile mechanical stress constantly promotes the growth of electrical trees along the electric field, whereas a temperature gradient accelerates this growth process. More damage accumulated during the growth process.

(2) Although compressive mechanical stress initially reduces the tree growth and accumulated damage, after the applied stress reaches 10 MPa, the process returns to inducing an increase in the tree length and damage, similar to the tensile mechanical stress. The temperature gradient also accelerates the process.

(3) The mechanical stress and temperature gradient simultaneously affect the electrical tree degradation process of the epoxy resin. When the mechanical stress increased from 20 MPa to 30 MPa, the stress was released at high temperatures, and the effect of temperature on the electrical tree was dominant.

(4) Both thermal and mechanical stresses must be emphasized when considering epoxy resin insulation for equipment. In this study, only vertical stress was applied to the sample. The applied stress in the horizontal direction must be investigated. Moreover, epoxy resin is cured with several catalysts and accelerators during the actual work process. Hence, it is difficult to observe the stress distribution using the current equipment setup, which needs to be improved in future studies.

References

[1] J Li, H Aung, B Du. Curing regime-modulating insulation performance of anhydride-cured epoxy resin: A review. *Molecules*, 2023, 28(2): 547.

[2] J Li, P Guo, X Kong, et al. Curing kinetics and dielectric properties of anhydride cured epoxy resin with different accelerator contents. *IEEE Transactions on Dielectrics and Electrical Insulation*, 2023, 30(1): 20-30.

[3] J Li, P Guo, X Kong, et al. Curing degree dependence of dielectric properties of bisphenol-a-based epoxy resin cured with methyl hexahydrophthalic anhydride. *IEEE Transactions on Dielectrics and Electrical Insulation*, 2022, 29(6): 2072-2079.

[4] C Chen, J Li, X Wang, et al. Transport characteristics of interfacial charge in SiC semiconductor-epoxy resin packaging materials cured with methyl hexahydrophthalic anhydride. *Frontiers in Chemistry*, 2022, 10: 879438.

[5] P Liu, H Zhang, S Zhang, et al. Space charge dynamics in epoxy resin under voltage polarity reversal at various temperatures. *High Voltage*, 2021, 6(5): 770-781.

[6] J Li, X Kong, B Du, et al. Effects of high temperature and high electric field on the space charge behavior in epoxy resin for power modules. *IEEE Transactions on Dielectrics and Electrical Insulation*, 2020, 27(3): 882-890.

[7] R Zhao, Y Chen, J Li, et al. Interface damage driven electrical degradation dynamics of glass fiber-reinforced epoxy composites. *Composites Science and Technology*, 2023, 233: 109921.

[8] J Li, S Liu, P Song, et al. Solidification dynamics of silicone oil and electric field distribution within outdoor cable terminations subjected to cold environments. *IEEE Transactions on Power Delivery*, 2023, 37(5): 4126-4134.

[9] W Zhao, X Xia, M Li, et al. Online monitoring method based on locus-analysis for high-voltage cable faults. *Chinese Journal of Electrical Engineering*, 2019, 5(3): 42-48.

[10] J Li, Y Wang, J Dong, et al. Surface charging affecting metal particle lifting behaviors around epoxy spacer of HVDC GIL/GIS. *IEEE Transactions on Dielectrics and Electrical Insulation*, 2022, 29(4): 1546-1552.

[11] E Tuncer, I Sauers, D R James, et al. Electrical insulation characteristics of glass fiber reinforced resins. *IEEE Transactions on Applied Superconductivity*, 2009, 19(3): 2359-2362.

[12] C Saxén, E K Gamstedt, R Afshar, et al. A micro-computed tomography investigation of the breakdown paths in mica/epoxy machine insulation. *IEEE Transactions on Dielectrics and Electrical Insulation*, 2018, 25(4): 1553-1559.

[13] X Ren, L Ruan, H Y Jin, et al. Electrical-mechanical model of electrical breakdown of epoxy-impregnated-paper insulated tubular busbar with bubble defects. *IEEE Access*, 2020(8): 197931-197938.

[14] T Liu, H Liu, J Liu, et al. An insulation breakdown fault caused by stress cracking of GIS basin insulators. *High Voltage Electrical Appliances*, 2020, 56(2): 240-245.

[15] P Hu, C Li, D Chen. Analysis and countermeasures for the cracking of epoxy sleeves at GIS terminals of cables. *Electric Power Engineering Technology*, 2017, 36(1): 102-105.

[16] W Li, C Zhang, X Yu, et al. Analysis and preventive measures for the explosion fault of 500 kV GIL three pillar insulators. *Electric Porcelain Lightning Arrester*, 2019(3): 221-227.

[17] W Song, Y Meng, C Men, et al. Study on the ultrasonic detection method for internal defects of insulation pull rods in circuit breakers. *International Conference on Condition Monitoring and Diagnosis*. Xi'an, China: IEEE, 2016: 385-387.

[18] J Su, B Du, J Li, et al. Electrical tree degradation in high-voltage cable insulation: Progress and challenges. *High Voltage*, 2020, 4(5): 353-364.

[19] L Li, J Gao, L Zhong, et al. Aging phenomena in non-crosslinked polyolefin blend cable insulation material: Electrical treeing and thermal aging. *Frontiers on Chemistry*, 2022, 10: 903986.

[20] Y Sekki. Initiation and growth of electrical trees in LDPE generated by impulse voltage. *IEEE Transactions on Dielectrics and Electrical Insulation*, 2002, 5(5): 748-753.

[21] L Zhu, B Du, J Su, et al. Electrical treeing initiation and breakdown phenomenon in polypropylene under DC and pulse combined voltages. *IEEE Transactions on Dielectrics and Electrical Insulation*, 2019, 26(1): 202-210.

[22] W Zhang, B Du, H Liang, et al. Competition between tensile and compressive stresses on electrical tree growth in epoxy resin. *IEEE 4th International Conference on Electrical Materials and Power Equipment* (*ICEMPE*), 07-10 May, 2023, Shanghai, China. IEEE, 2023: 1-4.

[23] J Li, S Liu, H Liang, et al. Study on non-uniformity and dynamic fracture characteristics of GIL tri-post insulators considering Al_2O_3 sedimentation. *High Voltage*, 2022, 8(4): 659-667.

[24] B Du, Y Zhang, X Kong, et al. Morphological feature analysis of electrical tree growth in epoxy resin under tensile and compressive stress. *IEEE Transactions on Dielectrics and Electrical Insulation*, 2022, 29(1): 343-346.

[25] J Li, Y Wang, S Liu, et al. Thermal-elastic free energy

driven electrical tree breakdown process in epoxy resin under temperature gradient. *Materials Today Communications*, 2022, 33: 104951.

[26] T Kobayashi, J Dally. A system of modified epoxies for dynamic photoelastic studies of fracture. *Experimental Mechanics*, 1977, 17: 367-374.

[27] P Jia. Experimental study on the interfacial residual stress of resin matrix composites. Tianjin: Tianjin University of Commerce, 2018.

Hein Htet Aung received his B.E. degree in Electrical Engineering from China Three Gorges University, Yichang, China. He is currently working towards his M.E. at the Key Laboratory of Smart Grid of the Education Ministry, School of Electrical and Information Engineering, Tianjin University, China. His research interests include high-voltage insulation, epoxy resin and residual stresses.

Yuhuai Wang was born in Inner Mongolia, China in 1997. He received the B.S. degree in Electrical Engineering from Inner Mongolia University of Technology in 2018. He has been pursuing a Master's degree at the School of Electrical and Information Engineering at Tianjin University since 2020. His main research interests include insulation and mechanical failures of GIS/GIL.

Jin Li (M'17**)** was born in Tangshan, China, in 1988. He received the B.S. and Ph.D. degrees in Electrical Engineering from Tianjin University, Tianjin, China, in 2012 and 2017, respectively.

From 2017 to 2019, he worked as a Postdoctoral Researcher at Tianjin University. From 2018 to 2019, he was a Visiting Researcher with Tokyo City University, Tokyo, Japan. He is currently an Associate Professor with the School of Electrical and Information Engineering, Tianjin University. His research interests include functionally graded materials, dielectric properties, and the failure mechanisms of epoxy insulation.

Ying Zhang was born in Baoding, China, in 1996. She received the B.S. degree in Electrical Engineering from Tianjin University, Tianjin, China, in 2022. She is currently an Assistant at the Baoding Technical College of Electric Power Skills Training Center of State Grid Jibei Electric Power Co., Ltd. Her research interests include the mechanism and performance improvement of epoxy resin insulation degradation.

Tatsuo Takada was born in Yamanashi, Japan, in 1939. He received the B.E. degree in Electrical Engineering from the Musashi Institute of Technology, Japan, in 1963 and M.E. and Ph.D. degrees from Tohoku University, Japan, in 1966 and 1975, respectively. He became a Lecturer, an Associate Professor, and a Professor at Musashi Institute of Technology in 1967, 1974, and 1987, respectively. He was a Visiting Scientist at MIT (USA) from 1981 to 1983 and a Consulting Professor at Xi'an Jiaotong University, China in 1995. He has undertaken several research projects on the development of advanced acoustic and optical methods for measuring the electric charge distribution in dielectrics. For example, investigating the space charge effect in solid dielectric materials, the dynamic surface charge distribution on solid dielectrics, and the electric field vector distribution in liquid insulating materials. He received a Progress Award from the IEE of Japan in 1996. He also received the Whitehead Memorial Award in 1999 for his pioneering work on PEA and gave an Award Lecture at the IEEE Conference on Electrical Insulation and Dielectric Phenomena (CEIDP). He received the Chen Jidan Award for his contributions in charge measurement and quantum chemical calculations and gave a plenary speech at the International Conference on Electrical Materials and Power Equipment (IEEE ICEMPE). He is a Life Fellow of IEEE.